



HAL
open science

New Light on Old Wisdoms on Molten Polymers: Conformation, Slippage and Shear Banding in Sheared Entangled and Unentangled Melts

Laurence Noirez, Hakima Mendil-Jakani, Patrick Baroni

► **To cite this version:**

Laurence Noirez, Hakima Mendil-Jakani, Patrick Baroni. New Light on Old Wisdoms on Molten Polymers: Conformation, Slippage and Shear Banding in Sheared Entangled and Unentangled Melts. *Macromolecular Rapid Communications*, 2009, 30, pp.1709 - 1714. 10.1002/marc.200900331 . hal-03840796

HAL Id: hal-03840796

<https://hal.science/hal-03840796>

Submitted on 6 Nov 2022

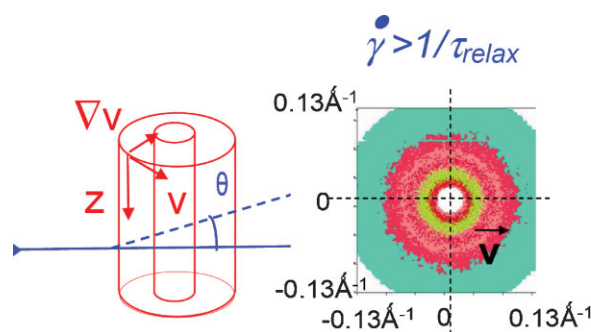
HAL is a multi-disciplinary open access archive for the deposit and dissemination of scientific research documents, whether they are published or not. The documents may come from teaching and research institutions in France or abroad, or from public or private research centers.

L'archive ouverte pluridisciplinaire **HAL**, est destinée au dépôt et à la diffusion de documents scientifiques de niveau recherche, publiés ou non, émanant des établissements d'enseignement et de recherche français ou étrangers, des laboratoires publics ou privés.

New Light on Old Wisdoms on Molten Polymers: Conformation, Slippage and Shear Banding in Sheared Entangled and Unentangled Melts

Laurence Noirez,* Hakima Mendil-Jakani, Patrick Baroni

The flow of viscoelastic materials is usually interpreted as resulting from intramolecular properties. Typically, the non-linear flow behaviour and sluggish relaxation dynamics in entangled polymers are interpreted by a disentanglement process. This molecular interpretation has never been validated by direct observation. We report here on in situ observations of polymer melts under steady-state shear flow using neutron scattering and particle tracking velocimetry. It is shown that the chains remain largely undeformed under steady-state shear flow whereas wall slippage and shear-banding are identified in both entangled and unentangled polymer melts. These observations are of prime importance; they reveal that the flow mechanism and its viscoelastic signature reflect a collective effect and not properties of individual chains.



Introduction

Some of the key questions relating to the flow mechanism of liquid polymers (melts) are: why do liquid polymers climb stirrer rods, why do they swell at the exit of an extruder and why do they produce spectacular instabilities (e.g., the “shark-skin” instability, gross melt fracture and Weissenberg effects^[1])? These relate in fact to how chains

move under flow at the temperatures at which they melt. The conventional molecular model (reptation)^[2] sees the chain as a snake-like tube that escapes from its environment. The flow is supposed to rearrange the tubes along the velocity direction when the flow rate $\dot{\gamma}$ becomes competitive with the molecule dynamic, i.e., when $\dot{\gamma} \geq \tau_{\text{relax}}^{-1}$ where τ_{relax} is the longest relaxation time of the chain. In the case of entangled chains, the relaxation time defines the reptation time, and the flow coupling to this relaxation time is supposed to give rise to an entangled-disentangled chain transition. This entangled-disentangled transition is the molecular interpretation of the non-linear transition to the shear thinning regime observed in rheology when the shear rate becomes higher than τ_{relax}^{-1} ^[2,3] (Figure 1(a)). However, to the best of our knowledge, no direct observation has shown that the shear thinning originates from a chain deformation. A wide panel of polymers^[4] exhibits excessive strain/

L. Noirez, P. Baroni
Laboratoire Léon Brillouin (CEA-CNRS), CE-Saclay, 91191 Gif-sur-Yvette, Cedex, France
Fax: 0033 1 6908 6300; E-mail: laurence.noirez@cea.fr
H. Mendil-Jakani
Structure et Propriétés d'Architecture Moléculaire, UMR 5819 SPram (CEA-CNRS-UJF), CEA-Grenoble, 17 avenue des Martyrs, 38054 Grenoble, Cédex 9, France

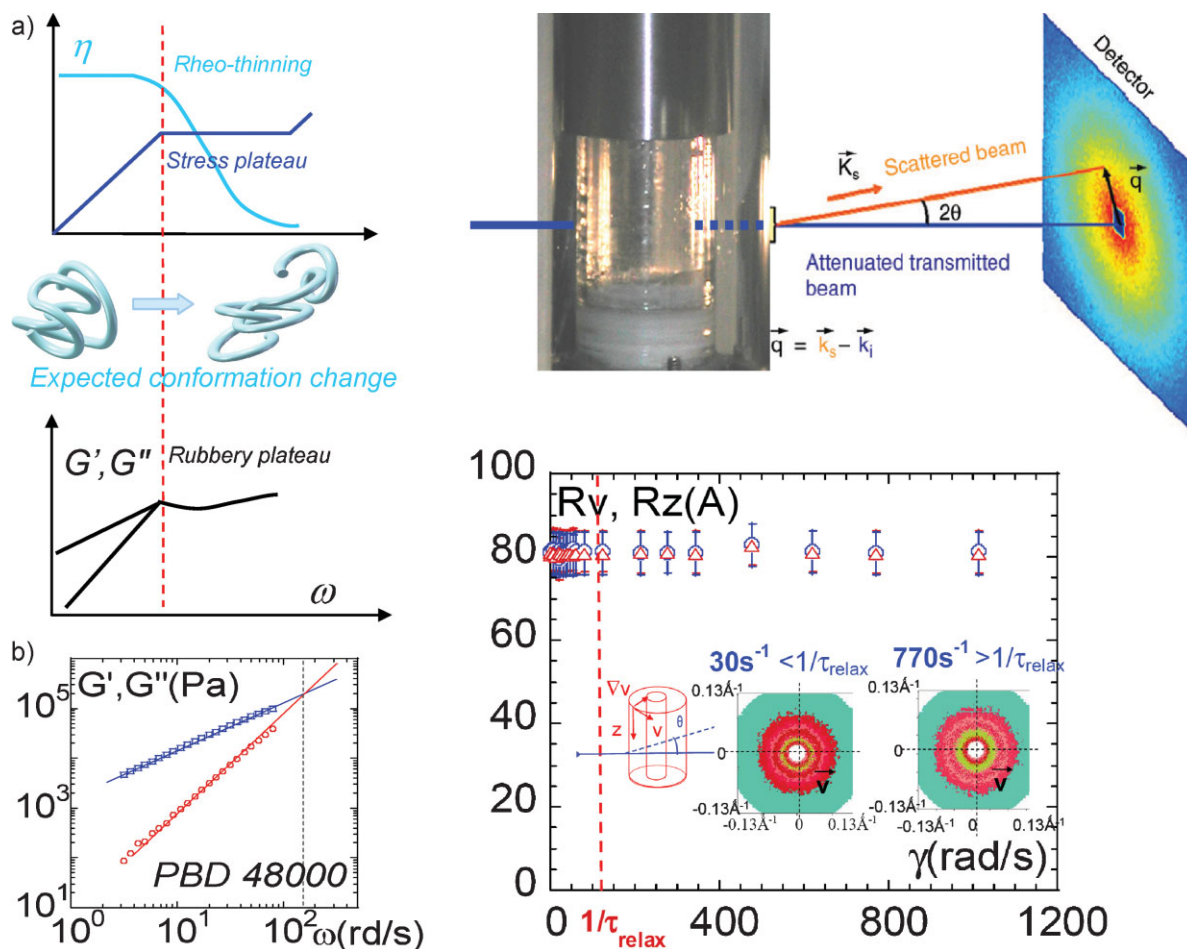


Figure 1. a) Scheme of the macroscopic rheological response of a polymer melt. The upper figure displays the viscosity η and the shear stress σ versus shear rate (flow curve). The rheofluidification zone (plateau) is interpreted by a shear-induced alignment of the chains. The bottom scheme shows the correspondence between the viscoelastic behaviour and the flow curve. The interception of the ω and the ω^2 scales of the viscoelastic curve defines the viscoelastic terminal time. b) Conventional dynamic relaxation measurement of the macroscopic terminal behaviour of the polybutadiene (PBD_{1,4}). The reptation time is $\tau_{\text{relax}} = 0.7 \times 10^{-2}$ s at 26 °C. The measurements were carried out in cone-plate geometry (20 mm diameter, 0.04 rad cone angle, strain amplitude 5%, aluminium fixtures). c) Photograph of the quartz Couette cell (diameter: 18 mm, thickness: 0.1 mm, shear rate: 500 s⁻¹). The PBD melt fills the Couette cylinder. The horizontal lines in the melt show that it is strongly stressed. d) Evolution at room temperature of R_v and R_z the components of the radius of gyration of the PBD_{1,4} following the velocity (v) and the neutral axis (z) respectively, versus shear rate (Couette geometry, quartz surfaces, gap thickness 1 mm). The insets show the 2D scattering patterns observed at 30 s⁻¹ and 770 s⁻¹ corresponding to shear rates respectively below and above the conventional terminal relaxation time of the polymer.

shear softening that cannot be explained on the basis of a chain alignment. Unexpected macroscopic instabilities,^[1] large timescale relaxations^[5] and shear induced phase transitions^[6,7] also highlight important failures of the current understanding and motivates a direct observation of the chain *under steady-state shear flow*.

The present work focuses on the in situ description of polymer melts under steady-state shear flow. Molecular dimensions are probed using neutron scattering whereas micrometer length scales are examined using particle tracking velocimetry. Our finding contrasts with the commonly admitted scheme of a flow induced alignment of the chains above a critical shear rate coinciding with the

entangled-disentangled transition. We observed that the chains remain largely undeformed in the presence of shear flow for a wide range of shear rates, whereas wall slippage and shear-banding are identified in both the entangled and unentangled melts. This experimental observation, which invalidates the common wisdom, is however coherent with other data such as the fluorescence measurements from Bur on polybutadiene,^[8] rheo-NMR studies by Callaghan et al.,^[9] and SANS data for highly concentrated polymer solutions from Hammouda.^[10]

Small-angle neutron scattering presents the advantage that it gives access directly to the average conformational state of the chains.^[11] Associated with a shear set-up (Rheo-

SANS), this technique provides in situ information on how the flow field is transmitted to the melt at a molecular scale. The literature reports on steady-state Rheo-SANS carried out on diluted,^[12] semi-dilute and concentrated solutions of high molecular weight polymers^[12,10] or blends^[13] mainly studying induced phase separation effects. But to the best of our knowledge, the simple case of ordinary polymer melts submitted to a steady-state shear flow has not been specifically examined, although it is the relevant study to justify rheological interpretation in terms of an entanglement-disentanglement transition. SANS studies on polymer melts under steady-state flow are certainly scarce due to the difficulty of the experiments. Highly entangled materials are very viscous and exhibit strong non-linear behaviours that lead to expulse the fluid as typically in the case of the transient Weissenberg effect.^[1] To avoid the transition to an unstable flow regime, we study the behaviour of intermediate molecular weights far from the glass transition (T_g). These melts have the consistency of oil and flow readily.

The amorphous melts studied here are an entangled polybutadiene ($\bar{M}_w = 30$.Me) characterised by a terminal relaxation time of $\tau_{\text{relax}} = 0.7 \times 10^{-2}$ s (Figure 1(b)), and a low molecular weight (unentangled) polybutylacrylate ($\bar{M}_w < 2$.Me), characterised by $\tau_{\text{relax}} = 10^{-3}$ s.^[14] Both melts are monodisperse and sheared at room temperature (i.e., about 100 °C over T_g). The characteristics of the samples are summarised in Table 1.

Experimental Part

Rheo-SANS measurements were carried out on a 2-dimensional detector (Paxy of the Lab. Léon Brillouin) equipped with a Couette shear cell (0.1 mm gap, Quartz (Herasil II) surfaces)^[15] filled with a 1:1 hydrogenated/deuterated mixture of polymer chains (obtained by evaporation from a THF solution). The isotopic mixture creates a scattering contrast to visualize the molecular form factor.^[16] Figure 1(c) illustrates the geometry of the experiment. The plane probed by the neutron beam is the (v,z) plane containing the velocity and the axis perpendicular to both velocity and velocity gradient (neutral axis, called also vorticity). The measurements are carried out *in situ* integrated over about 1 h of acquisition time; they describe stationary shear states.

The chain dimensions are determined in the Guinier regime using a 2-dimensional fit of the 2-dimensional form factor:^[17]

$$I(q) = \frac{I_0}{1 + q_v^2 \cdot R_v^2 + q_z^2 \cdot R_z^2} \quad (1)$$

where q is the scattering vector and R_v and R_z , the components of the radius of gyration along the velocity and the neutral axis respectively.

The particle tracking velocimetry (PTV) technique uses the displacement of small particles (micrometer tracers) to visualize the fluid motion.^[18] The observation is carried out with a microscope in the (velocity, neutral axis) plane (Linkam cell) between two quartz (Herasil II) disks. The depth is defined by focussing the objective at different heights. Snapshots (captured with a CCD camera with 1/500 s speed) are taken as a function of depth and applied shear rate. The correct choice of the particles is essential to guarantee a velocity representative of the molecular displacement. Alumina particles of relatively monodisperse 4 μm diameter are chosen to ensure an optimum boundary interaction (total wetting) with the melt (hydrogenated melt) and are used in low concentration (<2 vol.-%). The velocity of individual particles is determined using a direct cross-correlation calculation with a high resolution algorithm.^[18] This method measures the similarity of displacement of a series of particles (typically the displacement of about 20 particles at each height is considered), Figure 2 illustrates the experimental geometry and a snapshot photograph of the (velocity, neutral axis) plane of the seeded melt. The narrow width of the coefficient of the cross-correlation peak guarantees that the particle set executes a uniform translation displacement in the plane of observation (and thus guarantees that the flow regime is laminar).

Results and Discussion

The rheo-SANS results are displayed in Figure 1(d). The radii of gyration R_v and R_z of the entangled polybutadiene are plotted as a function of the applied shear rate. The insets of Figure 1(d) show the two-dimensional (velocity, neutral axis) polymer form factor at low and at high shear rate. The visual observation shows the sheared state of the liquid (Figure 1(c)). No significant deviation from an isotropic shape (within the error bars) is observed, even at high shear rates. This result is unexpected in view of the wide shear rate interval explored (from 0.1 s⁻¹ to 1 015 s⁻¹) recovering

Table 1. Characteristics of the two polymers under study.

Polymer : (Supplier: Polymer Source) Me: entanglement molecular weight Tg: glass transition temperature	Polybutadiene PBD Me = 1600 Tg = -110 °C		Polybutylacrylate PBuA Me = 22 000 Tg = -64 °C	
Weight average molecular weight (\bar{M}_w in g·mol ⁻¹)	H species 46700	D species 48500	H species 25700	D species 23500
Polydispersity I	1.11	1.08	1.08	1.10

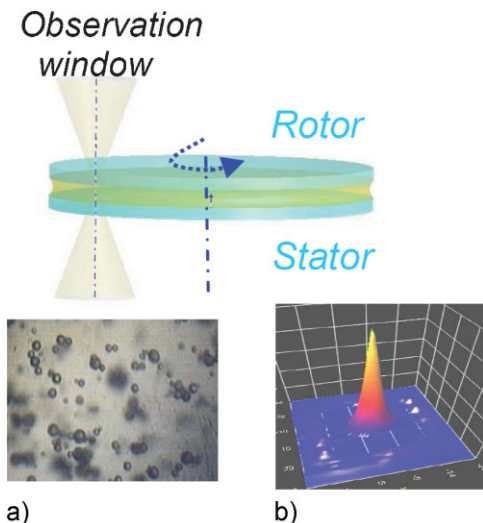


Figure 2. Geometry of the PTV measurement. The bottom left photo (a) is a snapshot of the (velocity, neutral axis) plane of the melt seeded by particles. The bottom right picture (b) shows a 3D representation of the result of the calculation of the coefficient of cross-correlation peak. The position of the peak indicates the average displacement of the particles and the width measures the degree of correlation between particle displacements. The uniformity of the particle translation displacement (narrow width of the peak) guarantees that the flow regime is laminar.

the rate of the terminal relaxation time (the reptation time is $\tau_{\text{relax}} = 0.7 \times 10^{-2}$ s). The absence of chain deformation is also observed on low molecular weight polybutylacrylate sample. Its terminal relaxation time is $\tau_{\text{relax}} = 10^{-3}$ s. The highest shear rates applied ($\dot{\gamma} \approx 800 \text{ s}^{-1}$) correspond to frequencies where a flow coupling is possible. Rheo-SANS experiments on polybutadiene and on polybutylacrylate thus show that in both cases the macromolecules are on average not oriented under flow. The absence of deformation suggests that the shear stress is not transferred to the melt. It supposes that a slipping zone is created as soon as the lowest shear rates.

To examine how the shear is transmitted to the fluid, an in situ observation of the velocity profile was carried out. Polybutylacrylate and polybutadiene are supposed to behave as simple liquids at low shear rates at room temperature (which corresponds to 90 and 135 °C above the glass transition respectively). Their velocity profile (at shear rates much smaller than τ_{relax}^{-1}) is expected to be linear. A deviation from the linearity implies that forces other than entanglements provide a resistance to the flow.

We first determined the velocity profile of the entangled polybutadiene. The applied shear rates were from 5 to 50 times below the rate of the viscoelastic terminal time ($\tau_{\text{relax}} = 0.7 \times 10^{-2}$ s). The resulting velocity profile determined in the flow gap at different shear rates (Figure 3(a)) does not strictly follow the imposed linear velocity gradient. This is particularly visible in the inset of

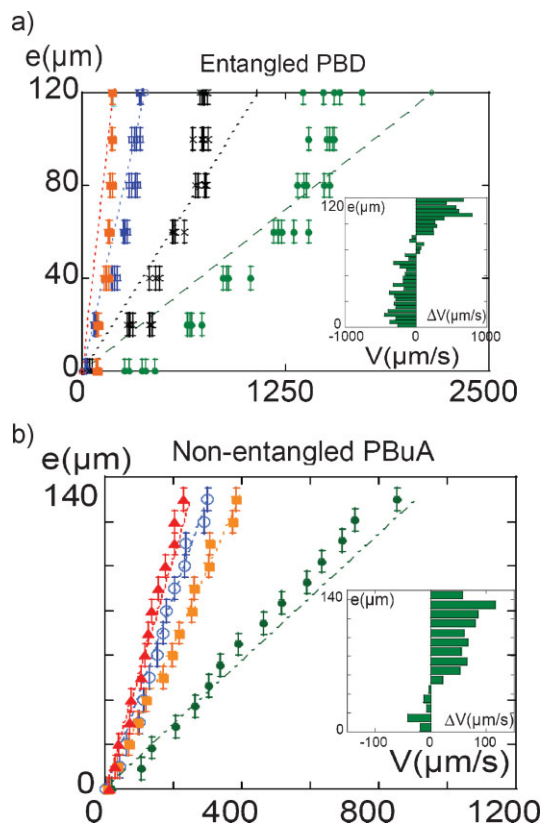


Figure 3. Velocity gradients displayed by the entangled polybutadiene (PBD_{1,4}) and the non-entangled polybutylacrylate (PBuA). The vertical axis corresponds to the gap thickness and the horizontal axis to the velocity. The dotted lines represent the imposed velocity gradients ($V_{\text{imp}} = \dot{\gamma} \cdot e$ where $\dot{\gamma}$ is the shear rate and e the gap thickness). a) PBD_{1,4} ($\bar{M}_w = 46\,700$, $\bar{M}_w > 2 \cdot \text{Me}$): (■): $\dot{\gamma} = 1.59 \text{ s}^{-1}$, (□): 3.23 s^{-1} , (X): 8.95 s^{-1} , (●): 17.9 s^{-1} . b) PBuA ($\bar{M}_w = 23\,000$, $\bar{M}_w < 2 \cdot \text{Me}$): (▲): $\dot{\gamma} = 1.9 \text{ s}^{-1}$, (○): 2.3 s^{-1} , (■): 3 s^{-1} , (●): 6.5 s^{-1} . The displacement is determined by observing the individual motion of about ten particles, over about 20–40 snapshots. The dispersion on the particle velocity is less than 1% and the error on the vertical position is about $\pm 5 \mu\text{m}$. The same measurement is repeated 3–4 times to ensure a stationary state description of the melt. The insets represent the velocity difference between the imposed and the measured values ($\Delta V = V_{\text{imp}} - V_{\text{meas}}$) versus gap thickness (e) for the highest shear rate. It points out wall slippages and fractures within the melt.

Figure 3(a), displaying the difference between the imposed and the observed velocities. The relative fluid/substrate velocity is not zero close to the moving and the static surfaces. The boundary condition does not hold even at rates much slower than any known relaxation time. These velocity discontinuities could not be associated with entanglement time scales ($\dot{\gamma} = 1.6 \text{ s}^{-1} \ll 1/\tau_{\text{relax}} = 143 \text{ s}^{-1}$). An abrupt change in the velocity gradient is also observable in the middle melt separating the sample into layers of different shear gradients (shear banding). Shear banding is a typical effect observed in worm-like micellar solutions. It

is analysed in analogy with the tube model of polymers as the instability generated when the time scale of the reptation is reached.^[19,20] The present experimental results rule out a flow coupling arising when $\dot{\gamma} \times \tau_{\text{relax}} > 1$. Both the low shear rate slippage regime and shear banding effects are unexpected since the entangled melt undergoes the shear field at rates much slower than the reptation time (at $\dot{\gamma} \times \tau_{\text{relax}} \ll 1$). If these instabilities do not originate from entanglements, low molecular weight systems (below the entanglement threshold) should also exhibit wall slippage and shear banding flow.

The second sample, the unentangled polybutylacrylate ($\bar{M}_w = 23\,000 < 2\text{Me}$), is typically described by a viscoelastic Maxwell model, with a terminal relaxation time of $\tau_{\text{relax}} = 10^{-3}\text{ s}$.^[14] The data points corresponding to the shear velocity (Figure 3(b)) are distributed systematically in advance or in delay with respect to the imposed shear field (dotted lines). The inset underlines the velocity difference between the imposed and the observed velocities as a function of the imposed velocity (i.e., the gap thickness). The deviation from the imposed shear field is observable from the lowest applied shear rates. It reveals a partial wall slip state occurring at rates much below any known relaxation time of the polymer. The creation of slipping zones and of shear banding is accelerated by increasing the shear rate. Upon shear cessation, particles exhibit first a fast motion decay followed by a slow relaxation,^[21] suggesting that these long range correlations are self-healing.

Conclusion

In this manuscript, we have presented new SANS measurements under steady-state flow on molten polymers together with PVT measurements carried out in total wetting boundary conditions. Both studies reveal important results. Polymer chains do not exhibit any deformation in the plane (velocity, neutral axis) from low shear rates up to values greater than the inverse of the reptation time. As already observed,^[22] PVT measurements reveal partial wall slippage, but also shear banding even at low shear rates. Partial wall slippage and shear banding are zones of stress dissipation. The slipping (the highest stress zones) is restricted to narrowly defined zones in the sample. It may explain why no deformation and *a fortiori* no entanglement-disentanglement transition are observed in the plane (velocity, vorticity) since the dissipation zones preserve the major part of the melt from the deformation and this, from the smallest shear rates. The other important point is that the partial slippage regime is occurring on timescales much longer than the terminal relaxation time. It suggests that the melt may contain very long (intermolecular^[20]) correlations. Recent dynamic relaxation developments tell that a significant terminal elasticity is

measurable far away from the glass transition.^[23–25] The corresponding long range correlations are much larger than those classically described by the viscoelastic approach (Rouse, reptation). This macroscopic elasticity may explain low shear rate wall slippages or shear banding observed in highly entangled melts^[26] and unpredictable large time scale relaxations.^[5,12,27] The absence of chain deformation in the plane (velocity, vorticity) goes against the simple picture of chains that transit homogeneously to an elongated state along the flow. These results are not the only data discrediting the homogeneous flow picture in melts. Simultaneous shear stress and fluorescence on polybutadiene melts have also revealed the invariance of the shape with respect to the shear flow,^[8] rheo-SANS on highly concentrated polymer solutions does not reveal any anisotropy,^[10] an NMR study in Couette geometry shows an ordering of the melt in stratified slip planes similar as a log-rolling instability known in liquid crystal^[9] corroborating the velocity profile displayed in the present particle tracking study. These in situ results describing the stationary steady-state of polymer melts invite us to take caution with rheology interpretation in terms of homogeneous chain elongation and/or homogeneous disentanglement mechanism. Slippage transitions, fractures indicate in contrast that dissipative processes are involved and therefore, that the shear stress is not integrally transmitted to the melt. These results show that the no-slip boundary condition which is at the centre of the current debates in microfluidic and at nanoscales^[28] holds also at the macroscopic scale and in the low shear regime. Therefore wetting properties and shear geometry play a role in the velocity profile (wall slippage) and the rheological signature.^[29] However, the boundary conditions do not explain the fracture observed within the melt that indicates the strong cohesion of the liquid. The cohesive character of the melt dominates with respect to the shear stress and to the wall interactions. This analysis does not hold for diluted solutions (where the elongation is observed), the cohesive character of the melt being lost by the dilution.^[12,30] Finally, the present experiments do not have to be compared to transient effects (long step deformation, stretching,^[31] non-equilibrium quenched systems) that may exhibit a chain elongation but do not represent a stationary state.

Received: May 13, 2009; Accepted: June 10, 2009; Published online: August 11, 2009; DOI: 10.1002/marc.200900331

Keywords: interfaces; neutron scattering; rheology; shear; surfaces

- [1] [1a] M. D. Graham, *Chaos* **1999**, *9*, 154; [1b] S. Kim, J. M. Dealy, *Polym. Eng. Sci.* **2002**, *42*, 495; [1c] K. Weissenberg, *Nature* **1947**, *159*, 310.

- [2] [2a] P. G. de Gennes, "Scaling Concepts in Polymer Physics", Cornell University Press, Ithaca and London 1979; [2b] M. Doi, S. F. Edwards, "The Theory of Polymer Dynamics", Clarendon Press, Oxford 1986; [2c] G. Marrucci, N. Grizzuti, *Gazz. Chim. Ital.* **1988**, *188*, 179; [2d] M. E. Cates, T. C. B. McLeish, G. Marrucci, *Europhys. Lett.* **1993**, *21*, 451.
- [3] [3a] J. D. Ferry, "Viscoelastic Properties of Polymer", 3rd Edition, Wiley, New York 1980; [3b] P. Tapadia, S. Q. Wang, *Macromolecules* **2004**, *37*, 9083.
- [4] [4a] K. Osaki, M. Kurata, *Macromolecules* **1982**, *13*, 671; [4b] C. M. Vrentas, W. W. Graessley, *J. Rheol.* **1983**, *27*, 433; [4c] G. Marrucci, G. Ianniruberto, *J. Non-Newtonian Fluid Mech.* **1999**, *82*, 275.
- [5] [5a] S. Q. Wang, S. Ravindranath, P. Boukany, M. Olechnowicz, R. Quick, A. Halasa, J. Mays, *Phys. Rev. Lett.* **2006**, *97*, 187801; [5b] F. Boué, et al. *Prog. Colloid Polym. Sci.* **1987**, *75*, 152.
- [6] A. Romo-Uribe, C. D. Han, S. S. Chang, *Macromolecules* **1997**, *30*, 7977.
- [7] C. Pujolle-Robic, L. Noirez, *Nature* **2001**, *409*, 167.
- [8] A. J. Bur, R. E. Lowry, S. C. Roth, C. L. Thomas, F. W. Wang, *Macromolecules* **1991**, *24*, 3715.
- [9] P. T. Callaghan, M. L. Kilfoil, E. T. Samulki, *Phys. Rev. Lett.* **1998**, *81*, 4524.
- [10] B. Hammouda, A. I. Nakatani, D. A. Waldow, C. C. Han, *Macromolecules* **1992**, *25*, 2903.
- [11] J. S. Higgins, H. C. Benoit, "Polymers and Neutron Scattering", Oxford Science Publications, Oxford 1994.
- [12] [12a] P. Lindner, R. C. Oberthür, *Colloid Polym. Sci.* **1988**, *266*, 886; [12b] S. Saito, et al. *Macromolecules* **2000**, *33*, 2153; [12c] "Flow Induced Structure in Polymers", A. Nakatani, M. D. Dadmum, Eds., ACS Symp. Series, 1995, 597; [12d] T. Kume, T. Hashimoto, T. Takahashi, G. G. Fuller, *Macromolecules* **1997**, *30*, 7232.
- [13] R. S. Graham, J. Bent, N. Clarke, L. R. Hutchings, R. W. Richards, T. Gough, D. M. Hoyle, O. G. Harlen, I. Grillo, D. Auhl, T. C. B. McLeish, *Soft Matter* **2009**, *5*, 2383.
- [14] H. Lakrout, C. Creton, D. Ahn, K. R. Shull, *Macromolecules* **2001**, *34*, 7448.
- [15] P. Baroni, C. Pujolle, L. Noirez, *Rev. Sci. Instr.* **2001**, *72*, 2686.
- [16] J. S. Higgins, H. C. Benoit, "Polymers and Neutron Scattering", Oxford Science Publications, Oxford 1994.
- [17] G. Pépy, *J. Appl. Cryst.* **2006**, *40*, 433.
- [18] [18a] R. J. Adrian, *Ann. Rev. Fluid Mech.* **1991**, *23*, 261; [18b] R. J. Adrian, *Exp. Fluids* **2005**, *39*, 159; [18c] Program "DirectPIV 1.0" by R&D Vision; [18d] A. Sussey, J. M. Most, D. Honoré, *Exp. Fluids* **2006**, *40*, 70.
- [19] N. A. Spenley, M. E. Cates, T. C. B. McLeish, *Phys. Rev. Lett.* **1993**, *71*, 939.
- [20] [20a] M. E. Cates, S. M. Fielding, *Adv. Phys.* **2006**, *55*, 799; [20b] P. D. Olmsted, *Rheol. Acta* **2008**, *47*, 283.
- [21] In preparation.
- [22] [22a] V. Mhetar, L. A. Archer, *Macromolecules* **1998**, *31*, 8607; [22b] L. A. Archer, R. G. Larson, Y. L. Chen, *J. Fluid. Mech.* **1995**, *301*, 133.
- [23] B. V. Derjaguin, et al. *Polymer* **1989**, *30*, 97.
- [24] D. Collin, P. Martinoty, *Physica A* **2002**, *320*, 235.
- [25] [25a] H. Mendil, P. Baroni, L. Noirez, *Eur. Phys. J.* **2006**, *19*, 77; [25b] L. Noirez, P. Baroni, H. Mendil-Jakani, *Polym. Int.* **2009**, *58*, 962.
- [26] S.-Q. Wang, S. Ravindranath, Y. Wang, P. Boukany, *J. Chem. Phys.* **2007**, *127*, 064903.
- [27] [27a] P. Tapadia, S. Ravindranath, S. Q. Wang, *Phys. Rev. Lett.* **2006**, *96*, 196001; [27b] P. Tapadia, S. Q. Wang, *Phys. Rev. Lett.* **2006**, *96*, 16001.
- [28] D. M. Huang, C. Sendner, D. Horinek, R. R. Netz, L. Bocquet, *Phys. Rev. Lett.* **2008**, *101*, 226101.
- [29] Y. Woo Inn, K. F. Wissbrun, M. M. Denn, *Macromol.* **2005**, *38*, 9385.
- [30] A. Link, J. Springer, *Macromolecules* **1993**, *26*, 464.
- [31] [31a] K. Mortensen, O. Kramer, W. Batsberg, L. J. Fetters, *Mater. Res. Soc. Symp. Proc.* **1987**, *79*, 259; [31b] A. Blanchard, R. S. M. Heinrich, W. Pyckhout-Hintzen, D. Richter, A. E. Likhtman, T. C. B. McLeish, D. J. Read, E. Straube, J. Kohlbrenner, *Phys. Rev. Lett.* **2005**, *95*, 166001.